



## Molecular Crystals and Liquid Crystals Science and Technology. Section A. Molecular Crystals and Liquid Crystals

Publication details, including instructions for authors and  
subscription information:

<http://www.tandfonline.com/loi/gmcl19>

### Transitions to Ordered Phases in Systems Containing Rod-like Particles: III. Four Fundamental Reasons for the Predictive Deficiencies of Discrete Lattice Models

Larry A. Chick <sup>a</sup> & Christopher Viney <sup>b</sup>

<sup>a</sup> Pacific Northwest Laboratory, Richland, WA, 99352

<sup>b</sup> Center for Bioengineering, University of Washington, Seattle,  
WA, 98195

Version of record first published: 24 Sep 2006.

To cite this article: Larry A. Chick & Christopher Viney (1993): Transitions to Ordered Phases in Systems Containing Rod-like Particles: III. Four Fundamental Reasons for the Predictive Deficiencies of Discrete Lattice Models, *Molecular Crystals and Liquid Crystals Science and Technology. Section A. Molecular Crystals and Liquid Crystals*, 226:1, 63-86

To link to this article: <http://dx.doi.org/10.1080/10587259308028791>

PLEASE SCROLL DOWN FOR ARTICLE

Full terms and conditions of use: <http://www.tandfonline.com/page/terms-and-conditions>

This article may be used for research, teaching, and private study purposes. Any substantial or systematic reproduction, redistribution, reselling, loan, sub-licensing, systematic supply, or distribution in any form to anyone is expressly forbidden.

The publisher does not give any warranty express or implied or make any representation that the contents will be complete or accurate or up to date. The accuracy of any instructions, formulae, and drug doses should be independently verified with primary sources. The publisher shall not be liable for any loss, actions,

claims, proceedings, demand, or costs or damages whatsoever or howsoever caused arising directly or indirectly in connection with or arising out of the use of this material.

# Transitions to Ordered Phases in Systems Containing Rod-like Particles: III. Four Fundamental Reasons for the Predictive Deficiencies of Discrete Lattice Models

LARRY A. CHICK

*Pacific Northwest Laboratory, Richland, WA 99352*

and

CHRISTOPHER VINEY

*Center for Bioengineering, University of Washington, Seattle, WA 98195*

*(Received October 31, 1991; in final form July 24, 1992)*

This paper identifies and discusses four fundamental causes for the discrepancy between the entropy predictions of our new continuous-placement Monte Carlo (CMC) approach and the discrete lattice model (DLM) of Flory and Ronca. The DLM allows rods to cross, enables rods to fit too easily into tight spaces, does not account for unoccupiable (wasted) space, and neglects the ingrowth of short-range order. Increasing resolution can eliminate the first two shortcomings from the DLM. To account for wasted space in the DLM, it will be necessary to derive a more complex expression for combinatoric entropy. To properly accommodate the effect of short-range order, the calculation of both combinatoric and orientational entropy must be improved.

*Keywords: lattice model, Monte Carlo, rod-like particles, short-range order, two-dimensional, vacancies*

## INTRODUCTION

Comparisons in the previous paper<sup>1</sup> demonstrated that Flory's discrete lattice model (DLM)<sup>2,3</sup> thermodynamically "favors" short rods to an increasing degree at high concentrations and that, to a more minor extent, it "favors" disorder in monodisperse systems, but is a relatively good predictor of orientation distribution shape in monodisperse systems. In this paper, we examine four fundamental reasons why the DLM fails to accurately predict the fraction of occupiable vacancies, as determined by comparisons to continuous Monte Carlo (CMC) results from the model that was discussed in the first paper.<sup>4</sup>

Two of the problems with the DLM, that rods can cross and that it is too easy to fit rods into tight spaces, can be eliminated by increasing the resolution of the lattice. This technique is demonstrated in the following section. The third problem, that the lattice model does not account for unoccupiable (wasted) space, is discussed in the next section. The last problem that we identify, that the DLM fails to account for the ingrowth of short-range order, is addressed in the last section.

### Tight Spaces and Crossing Rods

That rods can cross through one another and that rods can be too easily placed in tight spaces in Flory's DLM are direct results of the use of a discrete lattice. These problems are not encountered in the CMC technique, which places rods with continuously varying positional coordinates.

Because the rods in the Flory lattice model are a single cell wide, the model does not preclude rods from crossing as shown in Figure 1. If vacant cells on either side of an existing rod share a common corner, they can be part of the trajectory of a new rod. (In three dimensions, the sequences at the crossing can also share an edge.) Obviously, rods that are perfectly aligned—comprised of a single sequence—cannot cross. The likelihood of rods crossing should be increased as the dispersion of the disorientations increases and should be maximum in an isotropic distribution. Also, as each rod becomes longer, its chance of intersecting another similar rod increases. In other words, an intersection can only involve cells that are not at the end of a rod, and the proportion of these cells increases with increasing axial ratio. So it appears that, by neglecting the effects of rods crossing, the DLM tends to overestimate the number of appropriate positions available to long rods and to rods in disordered configurations.

The second problem that can be directly attributed to the discreteness of the lattice model is that rods can touch or can be fit into tight spaces too easily, that is, with much higher probability than is justifiable in a real system. This problem is most clearly illustrated by reference to a one-dimensional system: Consider the

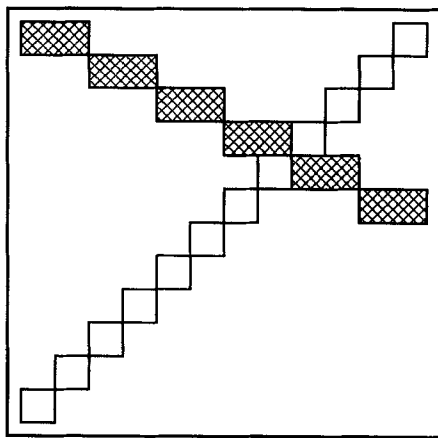


FIGURE 1 An example of how rods in the DLM can cross without any of their occupied cells overlapping.

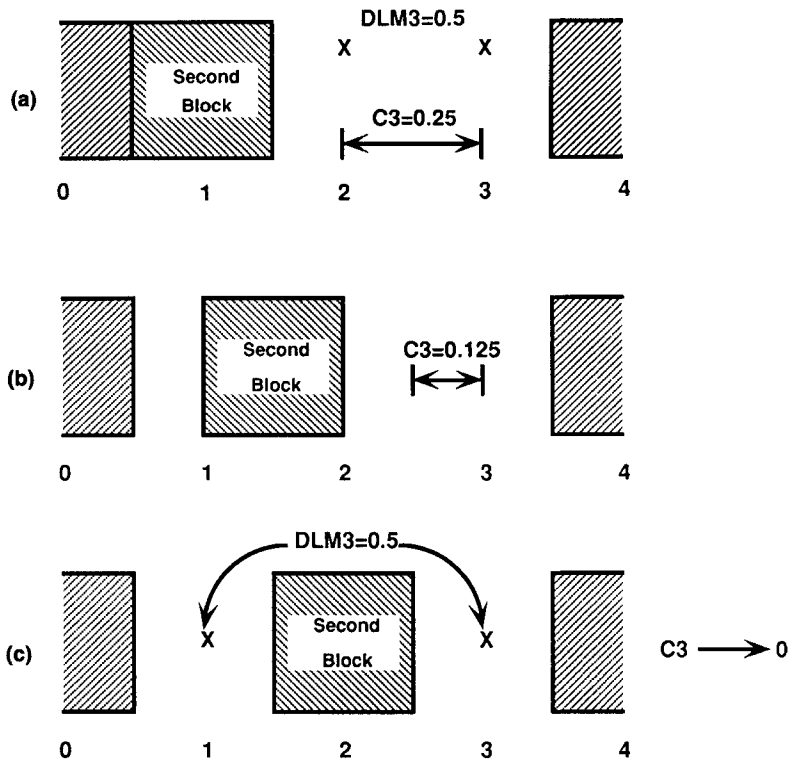


FIGURE 2 Three possible placements of the second block, resulting in a range of target sizes for the centerpoint of the third block. DLM3 is the probability of successfully placing the third block on any single attempt when discrete positioning is used. C3 is the probability of successfully placing the third block when continuum-type positioning is used.

problem of placing the third block in a row that is four blocks long, as shown in Figure 2. In all three situations that are shown, the first block has been placed such that it “wraps around” the periodic boundary. The three situations are created by different placements of the second block. In situation **a**, the second block has been placed next to one end of the first, leaving the maximum possible space for placement of the third block. If these blocks occupied discrete sites in a one-dimensional lattice, with placements possible at (exactly) 0, 1, 2, or 3 (4 is equivalent to 0 because of the periodic boundary), then the probability of successfully placing the third block in situation **a** would be  $2/4$  ( $DLM3 = 0.5$ ) signified by the two “X” symbols in the figure. In contrast, if the blocks were placed with continuous variation of position, then the centerpoint of the third block would have to fall in the range from 2 to 3 as signified by the arrow-tipped line, and the probability of successful placement would be 0.25 ( $C3 = 0.25$ ). Situation **b** could not happen in a discrete lattice, because the second block has not been placed exactly at an integer position. In situation **c**, the probability of successfully placing the third block into spaces just large enough to accommodate it, using a non-discrete choice of position, is vanishingly small ( $C3$  approaches 0). Yet if a discrete choice of position was used, then the placement probability would again be  $2/4$ , as it was in situation **a**.

In general, we can see that the DLM overestimates the ease with which a block can be fit into a "tight" space.

Rods fitting too easily into tight spaces result in overestimation of the combinatoric entropy by the DLM. This entropic term is related to the number of positions available at a given rod concentration divided by the number of positions available within the empty system. The empty system, having maximum positional freedom, is the proper reference state for  $S_c$ , just as the isotropic distribution is the proper reference state for the orientational entropy. Referring again to situation c in Figure 2, the DLM gives a 50% chance of the third block being placed. Yet out of the infinitely many possible ways of placing the block within the *continuous* empty system, there are exactly two possible ways of fitting the block in situation c. The resulting error in estimation of the combinatoric entropy can be substantial, as will be shown below.

### Development of the High Resolution Lattice Model for Perfect Alignment

Both the problem of rods crossing and of too easily fitting into tight spaces can be eliminated by altering the lattice model. Instead of using cells that are exactly the width of the rods, we increase the resolution of the lattice, such that rods are many cells wide. We have derived the model for the limiting case of perfectly aligned rods. Because the perfectly aligned rods cannot cross, even in the Flory DLM, our comparisons between lattice models will only reveal the errors due to easy fitting into tight spaces. Effects due to wasted space are not compensated for by either lattice model.

Figure 3 compares the ways perfectly aligned rods are represented in the discrete and in the high resolution lattice models (HRLM). A rod in the HRLM is  $r$  cells wide and  $l$  cells long. Therefore, its axial ratio,  $x$ , is:

$$x = l/r \quad (1)$$

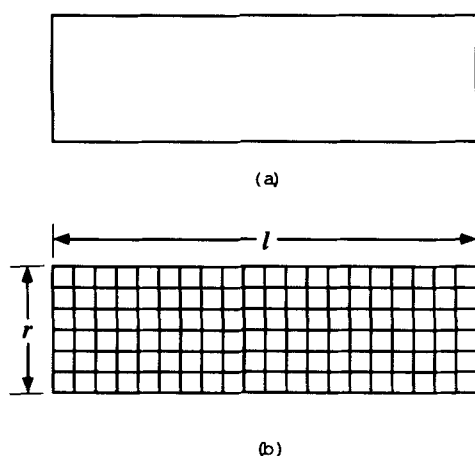


FIGURE 3 Comparison of the representation of perfectly aligned rods in (a) the discrete lattice model, and (b) the high resolution lattice model.

As with Flory's model, we use  $n_0$  for the total number of cells in the lattice,  $n_x$  for the number of rods, and  $n_1$  for the number of vacant cells.

We derive the placement probability,  $P$ , equal to the fraction of appropriate vacancies,  $v/n_0$ , in a manner similar to that used by Flory.<sup>1</sup> The nomenclature of cells for the HRLM is diagrammed in Figure 4. We start by developing  $P$  for the first cell. Then we develop  $P$  for each of the (equivalent) cells in the first column. These are combined into one term for placement of the first column. Similarly, we develop  $P$  for each of the cells within the first row, again combining into a single term. Finally, we derive  $P$  for the remaining (body) cells. The choice of which corner to assign to the first cells is arbitrary, as long as the rod is built up by moving consistently away from (in this case, up and to the right of) the first cell. The result is a four term expression that can be simplified based on several reasonable assumptions.

Consider the probability of successfully placing the very first cell, which is the lower left corner cell in the HRLM rod. As with Flory's first cell,<sup>1</sup> we have:

$$P_{\text{first cell}} = \frac{\# \text{ vacancies}}{\text{total } \# \text{ sites in lattice}} = \frac{n_1}{n_0} \quad (2)$$

Once the first cell has been placed, the conditional probability of successfully placing the next cell up in the first column is:

$$P_{1^{\text{st}} \text{ column cell}} = \frac{\# \text{ vacancies}}{\# \text{ vacancies} + \# \text{ first row cells}} = \frac{n_1}{n_1 + n_x} \quad (3)$$

This expression results from the fact that, once the first cell has been placed, the only types of cells that can physically exist in the next site up are either vacancies or cells within the bottom row of an existing rod, as shown in Figure 5. Since there are  $(r - 1)$  equivalent cells remaining within the first column of the rod, the consolidated  $P$  for the remainder of the first column is:

$$P_{1^{\text{st}} \text{ column}} = \left( \frac{n_1}{n_1 + n_x} \right)^{(r-1)} \quad (4)$$

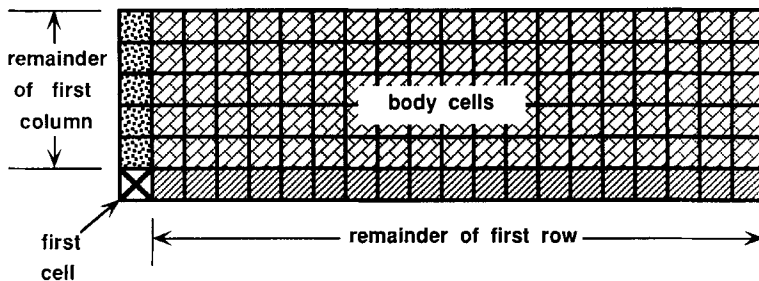


FIGURE 4 Nomenclature for the various classes of cells in the high resolution lattice model. Each class of cell—first cell, first column, first row, and body—results in a separate term for the probability of placing the rod.

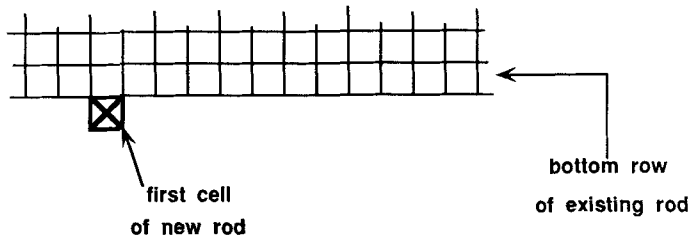


FIGURE 5 Diagram showing that the only type of cell that can block the placement of a first column cell—once the first cell has been placed—is a bottom-row cell of an existing rod.

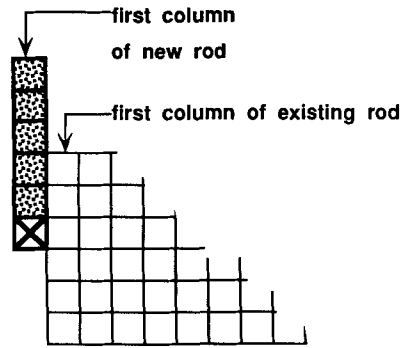


FIGURE 6 Diagram showing that the only type of cell that can block the placement of a first row cell is a first column cell of an existing rod.

Once the first column has been placed, we build the first (bottom) row. The remaining cells within the first row can only be blocked by a first column cell of an existing rod, as shown in Figure 6. Therefore,  $P$  for each of the remaining first row cells is given by:

$$P_{1^{\text{st}} \text{ row cell}} = \frac{\# \text{ vacancies}}{\# \text{ vacancies} + \# \text{ first column cells}} = \frac{n_1}{n_1 + rn_x} \quad (5)$$

and the consolidated term is:

$$P_{1^{\text{st}} \text{ row}} = \left( \frac{n_1}{n_1 + rn_x} \right)^{(l-1)} \quad (6)$$

Now the only remaining cells are the “body” cells. If we build these up from the inside corner made by the previous placement of the first column and row, then the only type of cell that can block placement is a lower left corner (first) cell of an existing rod. We have this situation for all body cells as long as we build out



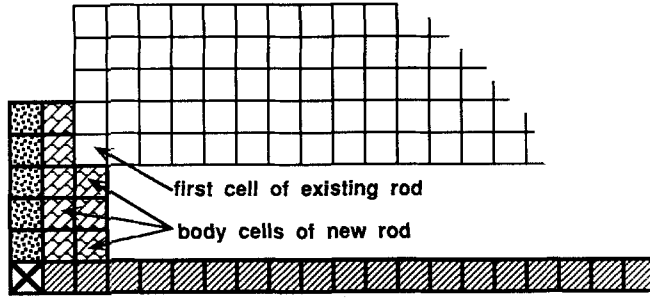


FIGURE 7 Diagram showing that the only type of cell that can block the placement of a body cell—when the body cells are added sequentially, building out and up from the inside corner—is a bottom-left-corner (first) cell of an existing rod.

from the inside corner, adding additional rows or columns in sequence, as shown in Figure 7. Then for each body cell we have:

$$P_{\text{body cell}} = \frac{\# \text{ vacancies}}{\# \text{ vacancies} + \# \text{ first cells}} = \frac{n_1}{n_1 + n_x} \quad (7)$$

and the consolidated  $P$  for the body is:

$$P_{\text{body}} = \left( \frac{n_1}{n_1 + n_x} \right)^{(r-1)(l-1)} \quad (8)$$

The probability for successfully placing the entire  $(n_x + 1)^{\text{th}}$  rod is:

$$P_{n_x+1} = \left( \frac{n_1}{n_0} \right) \left( \frac{n_1}{n_1 + l n_x} \right)^{(r-1)} \left( \frac{n_1}{n_1 + r n_x} \right)^{(l-1)} \left( \frac{n_1}{n_1 + n_x} \right)^{(r-1)(l-1)} \quad (9)$$

Now if we assume that the size of the lattice is vastly larger than the size of the individual rods, the probability for placing the  $n_x^{\text{th}}$  rod should be closely approximated by  $P$  for the  $(n_x + 1)^{\text{th}}$  rod, since the addition of one rod will barely increase the rod concentration:

$$P_{n_x} \approx P_{n_x+1} \quad (10)$$

Furthermore, if we increase the resolution of the model, so that each rod is made up of infinitely many cells, then we have:

$$r \approx r - 1, \quad l \approx l - 1, \quad rl \approx (r - 1)(l - 1) \quad (11)$$

Using these assumptions and taking logarithms, we have:

$$\ln P_{n_x} = \ln \left( \frac{n_1}{n_0} \right) + r \ln \left( \frac{n_1}{n_1 + l n_x} \right) + l \ln \left( \frac{n_1}{n_1 + r n_x} \right) + rl \ln \left( \frac{n_1}{n_1 + n_x} \right) \quad (12)$$

which can be rearranged to yield:

$$\ln P_{n_x} = \ln \left( \frac{n_1}{n_0} \right) - r \ln \left( 1 + \frac{ln_x}{n_1} \right) - l \ln \left( 1 + \frac{rn_x}{n_1} \right) - rl \ln \left( 1 + \frac{n_x}{n_1} \right) \quad (13)$$

Now, for large values of  $r$ ,  $l$ , and  $n_0$ , and for rod concentrations not too close to unity we have:

$$\frac{ln_x}{n_1} \ll 1, \quad \frac{rn_x}{n_1} \ll 1, \quad \frac{n_x}{n_1} \ll 1 \quad (14)$$

To very good approximation, the logarithm of one plus a small number is equal to that small number:

$$\ln(1 + \delta) \approx \delta \quad \text{for } \delta \ll 1 \quad (15)$$

Applying (15) to (13), we have:

$$\ln P_{n_x} = \ln \left( \frac{n_1}{n_0} \right) - r \left( \frac{ln_x}{n_1} \right) - l \left( \frac{rn_x}{n_1} \right) - rl \left( \frac{n_x}{n_1} \right) \quad (16)$$

The final three terms consolidate to give:

$$\ln P_{n_x} = \ln \left( \frac{n_1}{n_0} \right) - 3 \left( \frac{rln_x}{n_1} \right) \quad (17)$$

But for the area fraction or rod concentration in the HRLM, we have:

$$A_f = \frac{rln_x}{n_0} \quad (18)$$

and the total number of cells is given by:

$$n_0 = n_1 + rln_x \quad (19)$$

Finally, substitution and rearrangement results in the simplified expression for the logarithm of the fraction of appropriate vacancies for perfectly aligned rods in the high resolution lattice model:

$$\ln P = \ln \left( \frac{v}{n_0} \right) = \ln(1 - A_f) - \left( \frac{3A_f}{1 - A_f} \right) \quad (20)$$

Notice that the fraction-of-vacancies is not dependent on the axial ratio. Note also that increasing the resolution,  $r$ , of the lattice to infinity (11) effectively converts

the HRLM to a continuum basis, yet still preserves the straightforward lattice-type placement probability expressions.

### Discrete Lattice Model for Perfect Alignment

It is instructive to derive the special case of Flory's DLM for perfectly aligned rods. In this case, the rods are one cell wide and the number of cells in a rod is equal to the axial ratio. The model is simplified from that of Flory due to the lack of disorientation.

As before, for the very first cell we obtain:

$$P_{1^{\text{st}} \text{ cell}} = \frac{n_1}{n_0} \quad (21)$$

Each of the remaining cells can only be blocked by the first cell of an existing rod so that:

$$P_{\text{remaining cell}} = \frac{n_1}{n_1 + n_x} \quad (22)$$

and since there are  $(x - 1)$  such cells remaining:

$$P_{\text{remaining}} = \left( \frac{n_1}{n_1 + n_x} \right)^{(x-1)} \quad (23)$$

Then for the entire rod we have:

$$P_{n_x+1} = \left( \frac{n_1}{n_0} \right) \left( \frac{n_1}{n_1 + n_x} \right)^{(x-1)} \quad (24)$$

Using assumption (10):

$$\ln P_{n_x} = \ln \left( \frac{n_1}{n_0} \right) - (x - 1) \ln \left( 1 + \frac{n_x}{n_1} \right) \quad (25)$$

and approximation (15):

$$\ln P_{n_x} = \ln \left( \frac{n_1}{n_0} \right) - (x - 1) \left( \frac{n_x}{n_1} \right) \quad (26)$$

Rearrangement using (18) and (19) gives the result

$$\ln P = \ln \left( \frac{\nu}{n_0} \right) = \ln(1 - A_f) - \left( \frac{x - 1}{x} \right) \left( \frac{A_f}{1 - A_f} \right) \quad (27)$$

We can see that the vacancies available for perfectly aligned rods in the DLM depend upon the axial ratio. At  $x = 1$  the second term becomes zero. At very high axial ratios,  $(x - 1)/x$  approaches unity and the second term in (27) differs by a factor of three from that in the HRLM result (20).

### Comparison to Continuum Monte Carlo

Figure 8 shows three data sets from perfectly aligned CMC<sup>4</sup> for axial ratios of 1, 10, and 100. Within the margin of "noise," the curves are identical. It is evident that the fraction-of-vacancies for perfectly aligned rods does not depend on axial ratio.

Figure 9 shows a curve fit to the CMC data (labeled "Monte Carlo") along with results from the two lattice models, Equations (20) and (27). The high resolution model comes much closer to the CMC data than does the DLM, whose dependence on axial ratio is illustrated. The large gap in Figure 9 between the two lattice models can be directly attributed to the effect of overestimating the fraction-of-vacancies by allowing easy placement of rods into tight spaces.

It is evident, in Figure 9, that the DLM assigns short rods relatively larger vacancy fractions than it assigns long rods. However, because we have performed this comparison for the case of perfectly aligned rods, we cannot quantify the effect of changes in axial ratio on the errors due to tight fitting in the case of rods with disorientation. Nevertheless, it seems logical that the errors will always be more severe for short (fat) rods than for long (thin) rods: Think of infinitely thin rods; these should not tend to create "tight spots" due to their width, but only due to their length.

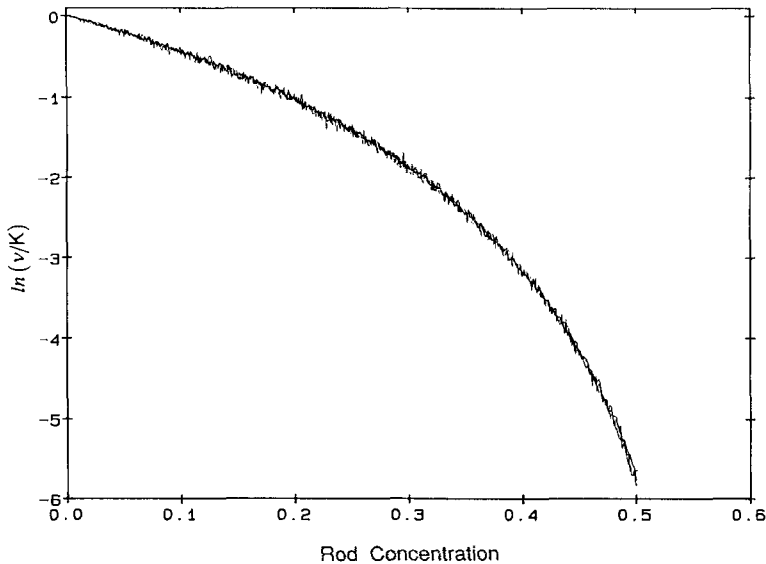


FIGURE 8 Three sets of vacancy fraction data from CMC on the placement of perfectly aligned rods. Data sets are for axial ratios of 1, 10, and 100. The three data sets are indistinguishable within the band of noise.

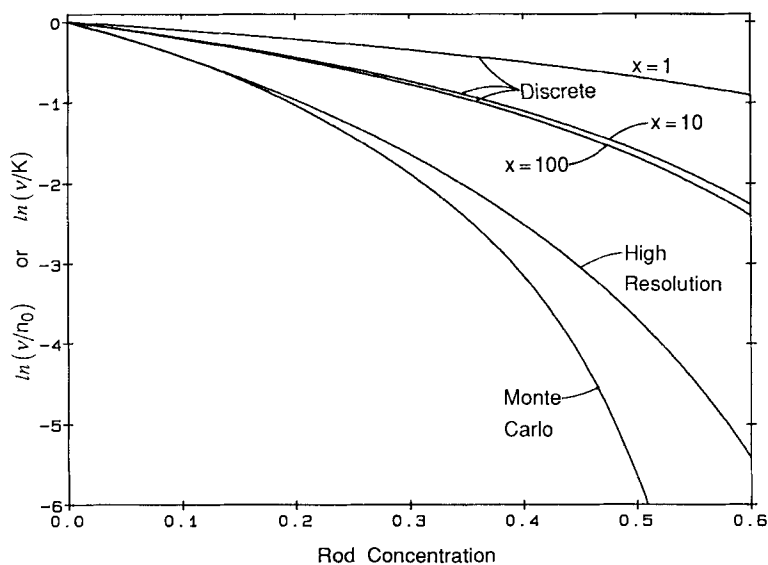


FIGURE 9 Fraction-of-vacancies for perfectly aligned rods predicted by the discrete lattice model (DLM) and by the high resolution lattice model (HRLM). Polynomial fit to the continuous Monte Carlo (CMC) data from Figure 8 is also shown. Only the DLM predictions are dependent on axial ratio.

The high resolution model dispels one of the major errors in estimation of the fraction-of-vacancies. Yet there is still a significant difference between the HRLM and the CMC results at high concentrations. This further problem is the subject of the next section.

### Wasted Space

As rods are added to the system, some of them will be placed sufficiently close to one another such that all or some of the space between them is "wasted"; that is, the space will be inaccessible to additional rods. This is why we have frequently used the modifiers, "appropriate" or "available" or "occupiable," when discussing the fraction-of-vacancies in rod configurations. Space is wasted in both DLM and continuous representations of rod configurations. The lattice models (both Flory's DLM and our HRLM) do not account for wasted space in the calculation of vacancies because the probability relations contain values for the total number of vacant cells, rather than the number of cells that are arranged contiguously such that they could be occupied by new rods. CMC effectively accounts for wasted space because rods simply cannot be placed where they cannot fit.

Flory and Irvine<sup>5</sup> discussed the existence of unoccupied space, discovered by comparing molecular dimensions to total system volume in neat liquids of poly-*p*-phenylenes, which are rigid rodlike molecules subject to orientation dependent mutual interactions. Their theory was adjusted to take wasted space into account by introducing a reduced volume term, the ratio of the volume occupied by the molecules to the total volume of the system. Critical temperatures were predicted by inserting the experimentally measured reduced volume into the theoretical re-

sults. Thus, although the theory compensates for wasted space, it is not explicitly accounted for in the predictions of vacancy fractions.

In Figure 2, situation **b**, the space to the left of the second block is wasted. In two-dimensional rod configurations that are generated by CMC, wasted space is generated between pairs of rods. Also, careful observation reveals that in many cases it is the interaction between more than two rods that creates wasted space. These space-wasting “multi-body” juxtapositions are evident in Figure 10, plotted from the CMC algorithm using perfect alignment and an axial ratio of unity. There are no occupiable vacancies remaining in this configuration, which has a rod concentration of 0.568. This means that slightly over 43% of the total space in this configuration is wasted and can never be filled by our CMC method.

### Wasted Space in One-Dimension

Whereas the wasted space in two-dimensional systems often occurs by multi-body interactions, that in one-dimensional systems is always due to simple pair-interactions, and is therefore much more easily quantified. CMC can be run such that, as blocks are placed in a row, the creation of wasted space is monitored. Figure 11 is a plot of the available space (line fraction) remaining as a function of block concentration. The available space curve is a polynomial fit to CMC data for repeated runs of the block placement algorithm. The linear function for total remaining vacant space is also shown. The area between the two lines represents the ingrowth of wasted space as the blocks are placed.

The occupiable space curve is “S shaped,” with a tail that asymptotically approaches zero useful space near a block concentration of 0.75. CMC runs were terminated only when there was no usable space remaining. As the configuration approached a concentration of 0.75, it was checked to detect and fill any remaining

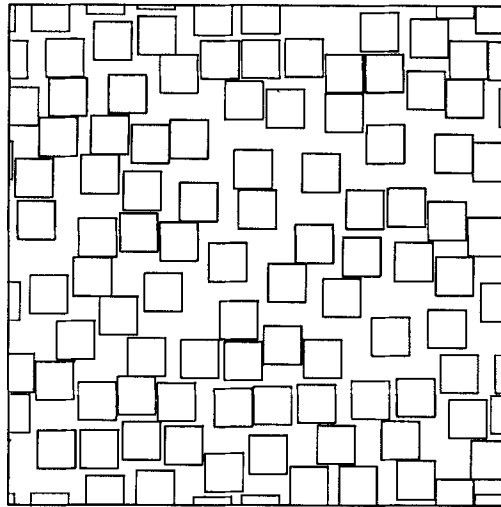


FIGURE 10 CMC-generated configuration of perfectly aligned rods with an axial ratio of unity. At an area fraction of 0.568, the configuration has reached terminal concentration; there are no occupiable vacancies remaining.

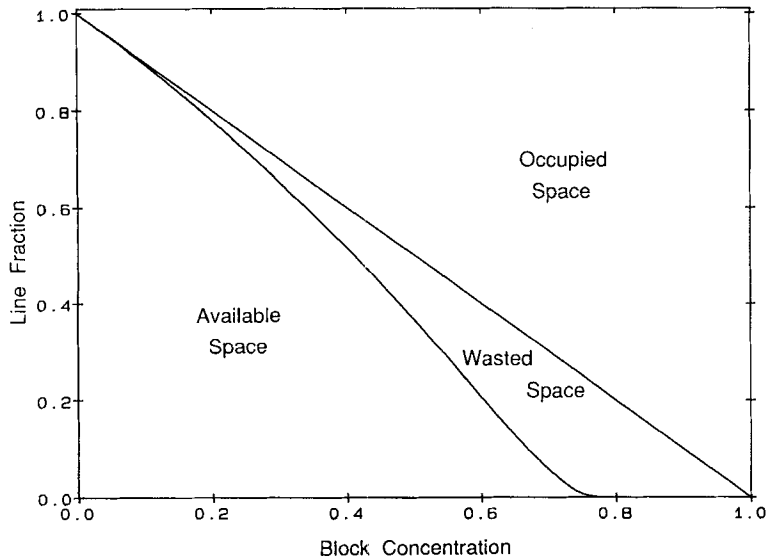


FIGURE 11 CMC-generated measurement of the ingrowth of wasted space as blocks are placed into a one-dimensional system, like that shown in Figure 2, but 500 blocks long. The upper line simply registers the space occupied by blocks as blocks are added. The lower curve is a measurement of the total line fraction comprised of occupiable vacancies (available space). At a given concentration, the distance between the two lines represents the ingrowth of wasted space, which is comprised of vacancies that are too narrow to accommodate a block.

usable vacancies. Because these last vacancies were barely larger than one block width, the fact that they were filled in a non-random fashion had no effect on calculation of the build-up of wasted space. The tail of the composite curve is due to the fact that some runs terminated before others. “Lucky” placement resulted in unusually high rod concentrations at termination, while “unlucky” placement resulted in an unusually high amount of wasted space at termination. The average of all runs gives the tail.

We believe that a rod concentration of 0.75 would be the overall average termination concentration for an infinite number of runs. Consider, for example, that continuum-type placement of the blocks in the four block long row depicted in Figure 2 will always result in a 75% fill at termination. Three blocks will virtually always be placed at termination because the probability of the second block landing such that it prevents placement of the third block (situation c) is vanishingly small. Similarly, placement of the second and third blocks such that there is (exactly) enough room for the fourth, followed by placement of the fourth into a space that is just large enough is exceedingly unlikely using continuous positioning.

Very little space is wasted at low block concentrations because blocks are rarely placed near to one another. As the block concentration is increased, the probability of new blocks being placed close to existing blocks also increases, accounting for the increasing negative slope of the available space curve at low to medium concentrations.

### Wasted Space in Two-Dimensions

Due to the complications of monitoring the ingrowth of wasted space when many-body interactions are involved, we have not monitored available space curves for the two-dimensional system. However, we have investigated the terminal area fraction by running CMC until no more rods are placed with 5 million tries. Figure 10 is typical of these runs for perfectly aligned rods. Based on these experiments, it appears that the terminal concentration for perfect alignment is very near 0.56 with no dependence on axial ratio. It is probably not fortuitous that 0.56 is the square of 0.75, the terminal concentration for the one-dimensional system.

Investigations of isotropic configurations have demonstrated that the terminal concentration is substantially lower than for perfect alignment. Randomly oriented rods with an axial ratio of 5 reach a terminal concentration near 0.47. It appears that the terminal concentration depends upon axial ratio for disoriented rods; isotropic configurations with an axial ratio of one reach a terminal concentration near 0.53. Therefore, we suspect that failure to account for wasted space will cause the DLM to favor disordered phases and short rods. (Again, recall the argument related to infinitely thin rods and tight spots. Similarly, thin rods should create less wasted space than do thick rods.)

### Implications of Wasted Space

Some additional comments can be made based on our investigation of the phenomenon of wasted space: It is apparent that the effects are minimal at low rod concentrations. This should hold for systems in one, two, or three dimensions. However, the effects may be extremely significant at high rod concentrations. The combinatoric entropy at high concentrations is apparently much lower than that predicted by the Flory lattice model, as indicated by Figure 9. Even the high resolution lattice model significantly overestimates the fraction of occupiable vacancies at high concentration.

The fact that our CMC runs reach a terminal concentration well below unity should, of course, not be construed as indicating rods cannot exist at higher concentrations. Our CMC method begins with an empty system, adding rods one at a time, and does not allow movement or consolidation. It is not impossible that a particular run would terminate at a substantially higher concentration than 0.56, only highly unlikely; rods would have to be placed close to one another throughout the build-up of the system. It is evident that the configuration shown in Figure 10 retains some positional entropy, even though it is at terminal concentration for our CMC placement. In this configuration, most of the rods can be slid in several directions, indicating that the system can be built up in many different ways. More rods could be fit into the configuration, but coordinated movement of the existing rods (such as that caused by compression) would be required to increase the rod concentration. So although it is evident that our CMC technique is not capable of measuring the entropy of highly concentrated systems, it is also evident that these systems have very low entropies relative to low density configurations. Therefore, relative to the empty system, the entropy at high concentration is much lower than that predicted by the DLM.



It is interesting to consider the implications of wasted space on a system containing a solvent component. In a real system, if the solvent molecules are isotropic, yet nearly the same size as the width of the rods, then it seems likely that wasted space will be present in the system even though the solvent molecules will fill most of the spaces between the rods. Such solvent particles could not fit into all of the inter-rod vacancies if the rods maintain true shape and are allowed continuously variable position and orientation. This casts further doubt on the validity of Flory's equation for the combinatoric entropy, Equation (7) in our previous paper,<sup>4</sup> in the case when a solvent is present. Flory assumed that this expression was valid either for a system of rods alone or for a system containing both rods and solvent molecules that were exactly the size and shape of single lattice cells. There is no additional problem for the latter system when it is represented by the DLM, because the solvent will fill all of the vacant cells between the rods. In that case, the positions of the indistinguishable solvent molecules will be determined solely by the positions of the rods, so that the combinatoric entropy of the system can be expressed as a function of the rod positions alone. In the real two-component continuum system, however, the solvent molecules may attain some additional positional freedom due to the presence of wasted space, necessitating the inclusion of an additional term to assess the true combinatoric entropy of the total system.

### Short-Range Order

Sheng<sup>6</sup> pointed out that the Onsager theory overestimates the magnitudes of density and order parameter discontinuities across the isotropic to nematic transition. He attributed the discrepancy to the theory's neglect of short-range order in the isotropic phase. Similarly, Warner<sup>7</sup> argued that neglect of short-range order by the Flory-Ronca model was indicated by its overestimation of both the latent entropy and the order parameter change in phase transitions of thermotropic liquid crystalline systems. Sheng attributes the cause of short-range order to the molecules' propensity to "bundle" due to attractive interactions, while Warner does not speculate on the cause.

Our CMC-generated configurations suggest that short-range order can be caused solely by space-filling constraints. Consider the rod configurations shown in Figure 12. In a global sense the orientations of the rods are isotropic, but the presence of clusters of roughly parallel rods is obvious. Frenkel<sup>8-14</sup>—who conducts the more common type of Monte Carlo experiments in which the particles are allowed to move, attaining an equilibrium configuration—also has demonstrated that configurations that may be isotropic on a global scale nevertheless contain significant degrees of short-range order, especially at high concentrations.

To understand why these clusters are formed in configurations that are isotropic on a global scale, consider the three stages of rod placement shown in Figure 13. At low concentrations (a) the rods "see" large areas of empty space and can be placed randomly in that space without restrictions on their orientation. But as more rods are added, the positions available to a new rod with a particular orientation become restricted to localities next to existing rods with similar orientation. Therefore, at high rod concentrations most new rods are placed into existing clusters because the most probable way to squeeze in more rods is to add to the clusters.

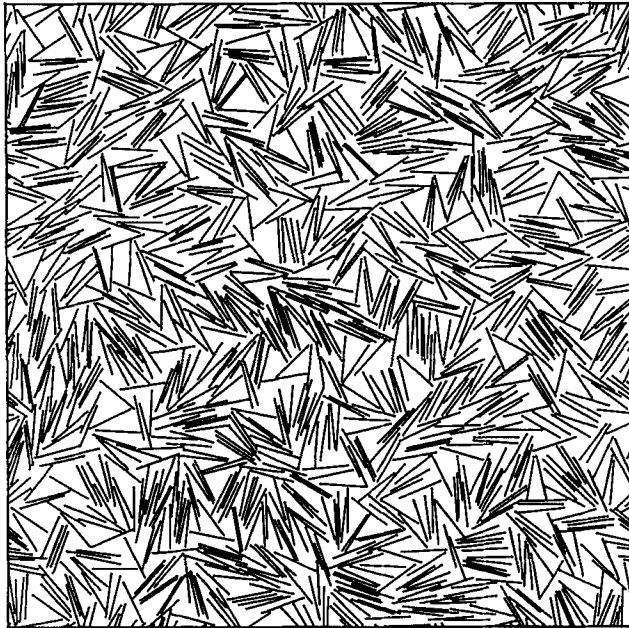


FIGURE 12 CMC-generated configuration of rods with axial ratio of 25 at a concentration of 0.263. The configuration is globally isotropic.

We have attempted to characterize the growth of these clusters by setting up rules to determine cluster membership. We say that rod A is clustered to rod B if the following three empirical conditions are met:

- a) the angle between them is less than  $15^\circ$ ;
- b) the distance between their midpoints is less than one half of a rod length; and
- c) the distance from the midpoint of either rod to the long axis of the other, measured along a direction perpendicular to the long axis of the first rod, is less than one fifth of a rod length.

(These conditions are stated exactly for infinitely thin rods; the rules become somewhat more sophisticated for rods with finite axial ratios.) To propagate the clustering relationship, we say that: if A is clustered to B, and B is clustered to C, then A is also clustered to C as long as the angle between A and C is less than  $15^\circ$ . The rules are somewhat arbitrary at this point, but result in computer-selected clusters which at least appear reasonable to the eye. The main point here is that the rules can be applied to obtain a relative measure of the degree of clustering in various rod configurations. Figure 14 shows the results of cluster membership measurements on CMC-generated configurations. It is evident that, as the rod concentration increases, the cluster size of the average rod increases ever more steeply. Furthermore, at a given rod concentration, cluster size is larger for the longer axial ratios.

Now refer to Figure 1 of the previous paper,<sup>1</sup> which shows vacancy fraction

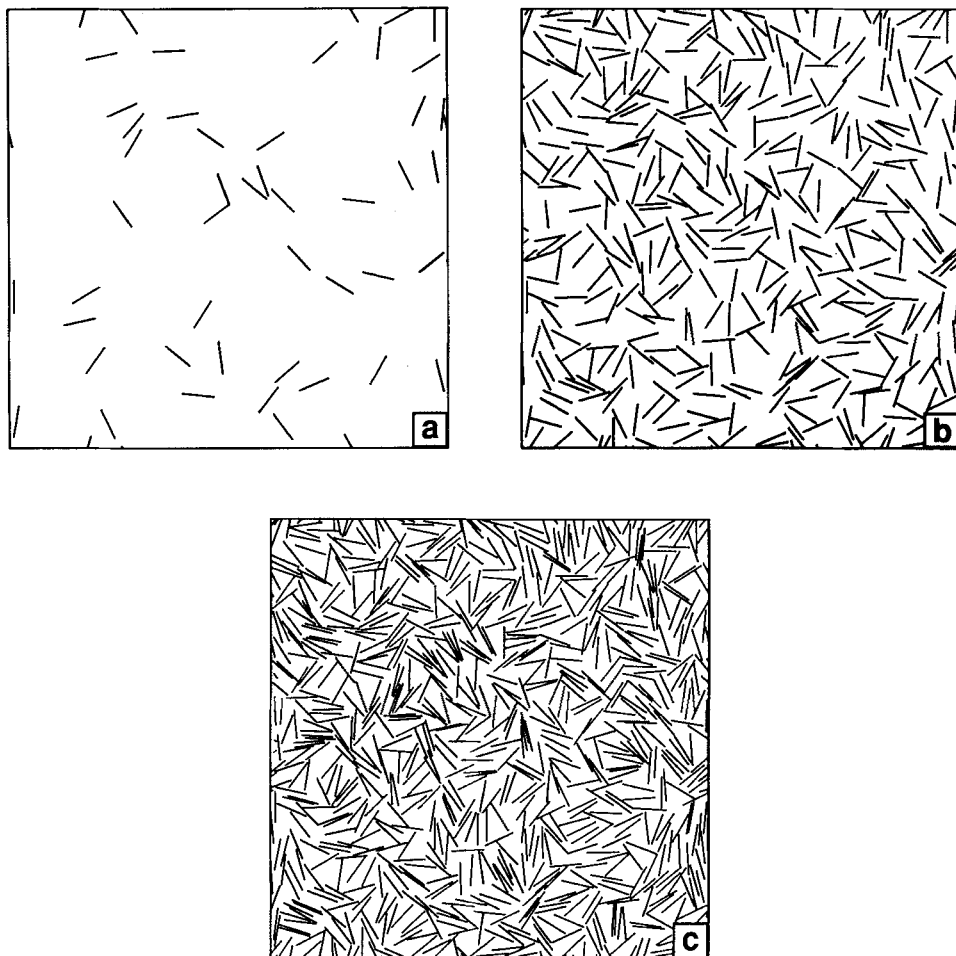


FIGURE 13 Three concentrations plotted from the CMC-generation of an isotropic configuration with  $x = 25$ : (a)  $A_f = 0.01$ , (b)  $A_f = 0.08$ , and (c)  $A_f = 0.16$ .

curves for isotropic configurations, generated by CMC (solid lines) and by the DLM (dotted lines). Notice that the CMC-generated curve for  $x = 100$  has an upward inflection that begins at about  $A_f = 0.04$ . The CMC curve for  $x = 25$  exhibits a less prominent inflection, while the CMC curve for  $x = 10$  has no apparent inflection. None of the DLM-produced vacancy fraction curves have inflections. Comparison to the data in Figure 14 shows that the inflections begin at a cluster membership size of roughly 2 to 3. The vacancy fraction curve in Figure 1 of the previous paper<sup>1</sup> for  $x = 10$  is terminated before it reaches a concentration corresponding to a cluster membership of 2.

We speculate that the inflections in the vacancy fraction curves are due to the ingrowth of clusters, which influence the dependence of vacancy fractions on concentration: At low concentrations, rods are added to what Flory would call a “mean field” of randomly oriented rods. At high concentrations the rods are added to a

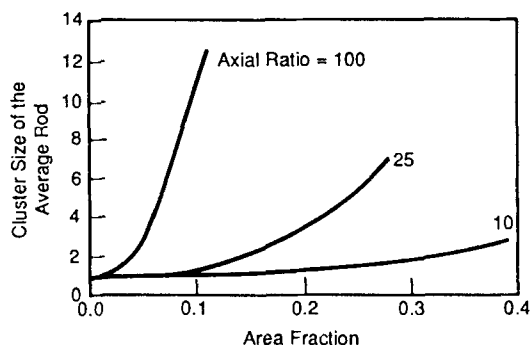


FIGURE 14 Plot of cluster size of the average rod as a function of rod concentration for isotropic configurations with three axial ratios.

configuration that cannot properly be characterized by Flory's mean field of disorder. Rather, these rods are added to an assemblage of clusters that resemble miniature aligned domains. At high concentrations, the rods must simply "find" the appropriately oriented cluster. Then the probability of successful placement within that cluster will be similar to the probability of placement within a globally aligned phase. If the rods were actually randomly oriented on a local as well as on a global scale (and they cannot be so arranged at high concentrations, due to space-filling constraints), we submit that the CMC-generated vacancy fraction curves would have no inflections; they would look more like the DLM-generated curves, which are based on the assumption of the maintenance of a mean field of disorder.

Note also, in Figure 3 of the previous paper,<sup>1</sup> that the CMC-generated vacancy fraction curve for the anisotropic configuration with a high degree of disorder ( $\sigma = 40^\circ$ ) has an inflection, but that the curve for the configuration which is well ordered on a global scale ( $\sigma = 10^\circ$ ) lacks an inflection, presumably because this configuration is essentially comprised of a single domain from the beginning.

The point is, it is easier to place rods into highly disordered configurations than might be expected, based on the mean field assumption of the DLM. Although local textures will occur even in globally ordered configurations (see Figure 17 of the previous paper<sup>1</sup>), the effects of not accounting for short-range order will tend to cause the DLM to underestimate the entropy of the isotropic phase relative to that of phases with global orientation; ordered phases will be favored. Also, as implied by Figure 14, when free energies of short rods are compared to those of long rods at similar concentrations, the neglect of short-range order will be more severe for the long rods, effectively favoring the short rods in the calculation of free energy.

## DISCUSSION

To appreciate the realism of the rod configurations that comprise the continuum "testing grounds" of our CMC technique, compare the "testing grounds" shown in Figure 15. In this figure, (b) is a CMC-generated plot of an isotropic configu-

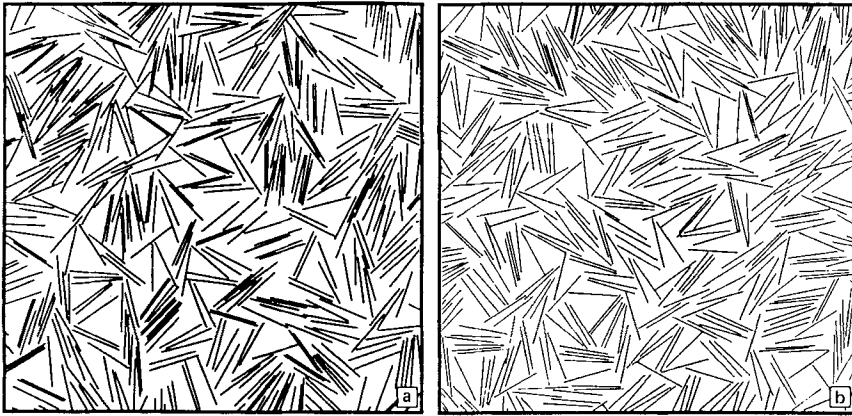


FIGURE 15 Comparison of: (a) Photo of wooden rods that were scattered onto a horizontal substrate, then vibrated until all lay flat on the surface. (b) CMC-generated representation of rods with the same axial ratio (25) and at the same rod concentration (0.263) as the configuration of wooden rods in (a).

ration, (a) is a photo of real wooden rods with the same axial ratio, 25, and at the same concentration, 0.263, as in the CMC configuration. The wooden rods were scattered onto a horizontal substrate, then the substrate was vibrated until all of the rods lay flat on the surface. The realism of the CMC-generated configurations should be compared to the approximations inherent in lattice treatments (see Figure 1 in Flory and Ronca,<sup>3</sup> Figure 1 in DiMarzio,<sup>15</sup> and Figure 1 in McCrackin<sup>16</sup>).

Our assertion is not that approximations and simplifications are of no use. Indeed, Flory's skill in knowing when and how to simplify the theoretical representation of natural phenomena was, perhaps, his best strength. Furthermore, we have already seen that our CMC approach is a blunt instrument, not useful at high rod concentrations. Monte Carlo of the type practiced by Frenkel<sup>8-14</sup> does attain high concentrations, but is restricted in its interpretation of the range of ordering and in its ability to determine the order of and the concentrations at which phase transitions occur. Also, continuum Monte Carlo techniques are limited in their ability to model systems with added complexity, such as rod flexibility and attractive forces. The magnitude of the required calculations becomes overwhelming. Therefore, sound theoretically-based models are essential for examination of the full range of rodlike particle systems. The main motivation for our work was to reveal the differences between the discrete lattice and the continuum representations of systems containing rodlike particles, with the hope that our discoveries might point the way for improving the predictive power of the DLM.

#### Proposed Improvements for the DLM

The choice of which improvements to incorporate into the DLM should be guided by its intended use. Errors in the DLM that can be shown by CMC experiments to offset one another may be tolerable for certain applications. However, it is well-known<sup>7,17-20</sup> that the DLM, as it stands, overestimates the degree of order of the anisotropic phase in the biphasic region. Also, we have shown that the DLM may be substantially untrustworthy for the treatment of polydisperse systems. When

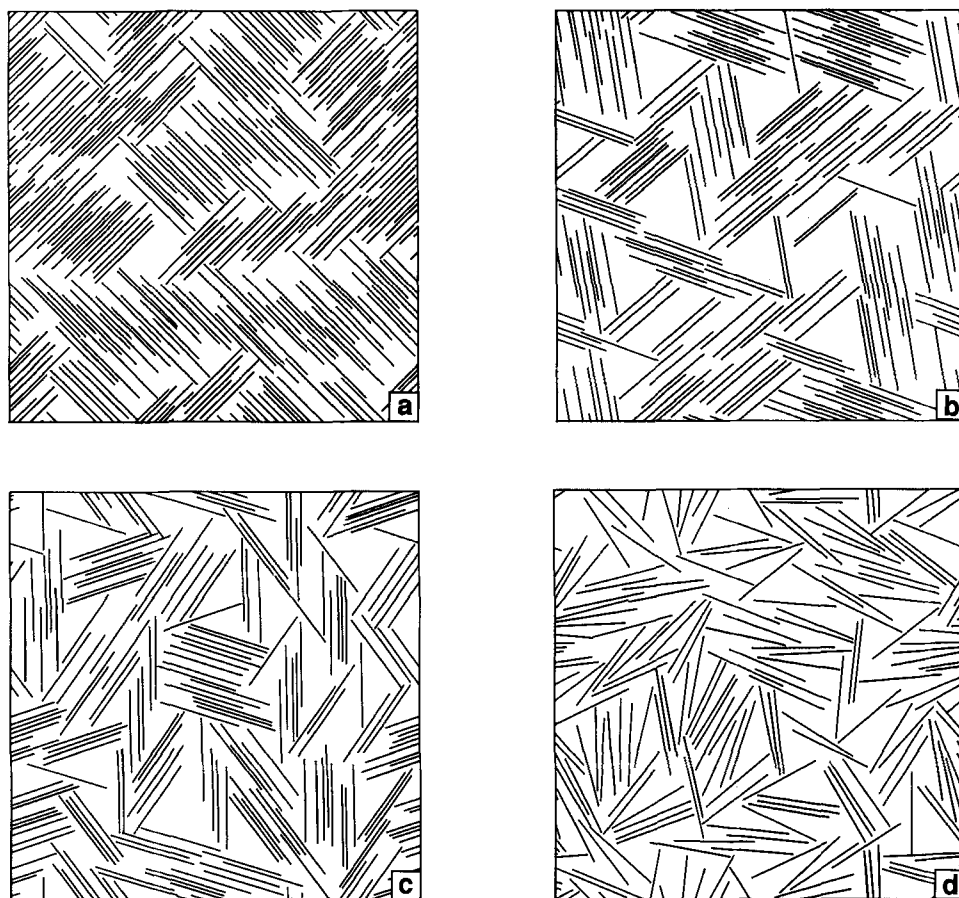


FIGURE 16 CMC-generated configurations with  $x = 25$ . Rods were placed using: (a) two possible orientations, (b) three possible orientations, (c) five possible orientations, and (d) infinitely many possible orientations (isotropic).

polydisperse systems undergo phase separation, it is well known<sup>21–26</sup> that the longer rods tend to congregate in the anisotropic phase while the shorter rods reside mainly in the isotropic phase. The DLM's relative overestimation of the vacancy fractions available to the short rods will then cause substantial underestimation of the free energy of the isotropic phase, and should result in erroneously high predicted transition concentrations. Our findings suggest several possible improvements, which could be combined or implemented separately, depending on the intended use of the model.

### Number of Sequences

We agree with Warner<sup>19</sup> that his alternate expression for the number of sequences gives an improved representation of the entropy of highly ordered phases. Any model that seeks a more accurate balance between order and disorder should incorporate this feature.











DLM Problem	Free Energy Balance	
Uses $y=x \sin \psi$	 Disorder Order	 Long Short
Allows <u>Rods to Cross</u>	 Disorder Order	 Long Short
Allows Easy Fitting in Tight Spots	 Disorder ? Order	 Long Short
Does Not Account for <u>Wasted Space</u>	 Disorder Order	 Long Short
Neglects <u>Short-Range Order</u>	 Disorder Order	 Long Short

FIGURE 17 Summary of the expected effects of problems with the DLM. The first column lists problems that we have identified with the DLM. The second column indicates whether the corresponding DLM problem predicts more disorder or more order in the anisotropic phase, compared to the prediction of CMC. The qualitative bias of the DLM is indicated by the balance, which “weighs” entropy and so slopes downward in the direction associated with decreasing free energy. The third column indicates whether the corresponding DLM problem overestimates entropy for long rods or for short rods. Again, the balance “weighs” entropy, and therefore slopes downward toward the condition associated with lower free energy.

### High Resolution Lattice Model

A high resolution lattice model (HRLM) would eliminate the problems of crossing rods and tight fitting. We demonstrated that the HRLM produces substantially improved estimates of vacancy fractions for perfectly aligned rods in two-dimensional systems. It should be possible to adapt the HRLM to rods with disorientation in both two- and three-dimensional systems. This would involve establishing a scheme to partition the HRLM rod into distinct groups of cells that can then be assigned appropriate placement probabilities. The relative numbers of these cell types (and therefore, the rod placement probability) would be functions of the rod disorientation.

### Accounting for Wasted Space

Wasted space should be accounted for by appropriately adjusting the pool of available vacancies that is used in the probability expressions of the DLM. The general shape of the function expressing the ingrowth of wasted space in one-dimensional systems, Figure 11, is certainly reasonable and can be expected to reflect the general shape of ingrowth for two- and three-dimensional systems. However we suspect that discovering the function that accounts for the combined effects of concentration, axial ratio and disorder on the ingrowth of wasted space will be a challenging problem.<sup>27</sup>

As we have demonstrated, it is beneficial to instigate the HRLM in order to clarify the effects of failing to account for wasted space; the use of CMC for comparisons to the HRLM should help guide the development of a wasted space correction.

### Accounting for Short-Range Order

Alben<sup>28</sup> concluded that “. . . The disagreements between theory (the DLM) and experiment are probably due to the long-range-order approximation and not to idealizations of the models. Thus the treatment of short-range-order, rather than more realistic models, appears to be the fruitful path for future research. . . .” We have shown that the DLM is inaccurate due both to the assumption of the mean field of disorder and to the “idealizations” of the model.

We have shown the effect of the ingrowth of short-range order on the vacancy fraction curves. However, we have not yet discussed the influence of short-range order on the orientational entropy. Do we overestimate  $S_o$  for the isotropic phase when we calculate it based on global disorder? It would seem so, based on the idea that the isotropic phase gets the “bonus” combinatoric entropy as a result of the ingrowth of clusters. Warner<sup>7</sup> argued that orientational entropy should be calculated on the basis of local, rather than global disorder, but he did not mention that short-range order should also be taken into account in predictions of the combinatoric entropy.

Let us consider briefly the implications of erecting a theory that does properly account for the effects of short-range order on both the orientational and the combinatoric entropies: We believe that such a theory could be used to predict the scale of the microstructure at equilibrium. We have reached this conclusion by observing that the independent variables that establish the state of a configuration of rods (axial ratio, concentration, and global orientation distribution) seem also to establish the scale of the microstructure. Figure 14 illustrates this quite clearly for the isotropic distribution. But we have also seen interesting inhomogeneities in the texture of globally aligned configurations (see Figures 16 and 17 of the previous paper<sup>1</sup> and the associated discussion). If the scale of the microstructure is established by those same parameters that determine the conditions of equilibrium, then the scale should be predictable.

We have restricted our investigations to rod configurations in which the shape and width of the global orientation distribution is imposed. This technique was chosen as being most appropriate for comparisons to the Flory approach. However, it should be possible to utilize the DLM (or HRLM) with the degree of short-range order imposed. The placement probability would be partitioned into two main terms, that for a rod to find a local neighborhood containing rods with similar angle to itself, and that for the rod to “move in” to the local cluster. The model would operate on the assumption of a mean field of clusters, rather than on a mean field of global order or global disorder.

We will end this discussion by offering one final set of CMC-generated configurations that may serve to stimulate ideas for modeling the scale of microstructures. We know that rods restricted to a single orientation will, by definition, produce a single domain. Figure 16 shows rods that were placed with (a) two possible orientations, (b) three possible orientations, (c) five possible orientations, and (d) infinitely many possible orientations. Note that the mean cluster size and the fraction of wasted space appear to be related to the number of available orientational states.



## CONCLUSIONS

With regard to the main motivation of these papers, to address the limitations of the discrete lattice representation in modelling the continuum, we have established that the DLM has several fundamental problems:

- a) Rods can cross in the DLM since they are represented as being one cell wide.
- b) The DLM underestimates the difficulty of fitting rods into tight spaces because it does not allow continuous positional variability.
- c) The DLM does not account for wasted space because it interprets all vacancies as being occupiable.
- d) Due to the assumption of a mean field of disorder, the DLM does not account for the ingrowth of short-range order in the isotropic phase as well as in anisotropic phases with relatively high degrees of global disorder.

It was also established<sup>1</sup> that these fundamental problems lead to errors in calculation of relative entropies:

- a) Short rods are assigned relatively higher entropies than are long rods, a problem that increases with increasing rod concentration.
- b) In the determination of phase equilibria for monodisperse systems, phases with high degrees of disorder are “favored” over phases with low degrees of disorder.

Based on our previous discussions of the severity of the DLM problems as a function of degree of order and axial ratio, we have produced the summary of “free energy imbalances” that is shown in Figure 17. The expected counterbalancing of the errors with regard to the predicted degree of order may account for the relatively minor inherent bias of the DLM toward disorder; the Flory-Ronca model achieves a delicate balance of errors when it is applied to monodisperse systems. However, the substantial favor of short rods is reflected by the last column of the figure.

## Acknowledgment

The authors wish to thank Pacific Northwest Laboratory, ACS-PRF (no. 21300-G7) and the I.B.M. corporation for financial support and Dr. A. Liebetrau for helpful discussions.

## References

1. L. A. Chick and C. Viney, *Mol. Cryst. Liq. Cryst.*, **226**, 25 (1993).
2. P. J. Flory, *Proc. Roy. Soc. London A*, **234**, 73 (1956).
3. P. J. Flory and G. Ronca, *Mol. Cryst. Liq. Cryst.*, **54**, 289 (1979).
4. L. A. Chick and C. Viney, *Mol. Cryst. Liq. Cryst.*, **226**, 63 (1993).
5. P. J. Flory and P. A. Irvine, *Chem. Soc. Farad. Trans 1*, **80**, 1807 (1984).
6. P. Sheng, *Introduction to Liquid Crystals*, Plenum Press, New York (1976).

7. M. Warner, *Mol. Cryst. Liq. Cryst.*, **80**, 79 (1982).
8. J. A. Cuesta and D. Frenkel, *Phys. Rev. A*, **42**(4), 2126 (1990).
9. D. Frenkel and R. Eppenga, *Phys. Rev. A*, **31**(3), 1776 (1985).
10. A. Stroobants, H. N. W. Lekkerkerker, and D. Frenkel, *Phys. Rev. Lett.*, **57**(12), 1452 (1986).
11. A. Stroobants, H. N. W. Lekkerkerker, and D. Frenkel, *Phys. Rev. A*, **36**(6), 2929 (1987).
12. D. Frenkel, *J. Chem. Phys.*, **91**(19), 4912 (1987).
13. D. Frenkel, *J. Chem. Phys.*, **92**(11), 3280 (1988).
14. J. A. C. Veerman and D. Frenkel, *Phys. Rev. A*, **41**(6), 3237 (1990).
15. E. A. DiMarzio, *J. Chem. Phys.*, **35**(2), 658 (1961).
16. F. L. McCrackin, *J. Chem. Phys.*, **69**(12), 5419 (1978).
17. P. G. de Gennes, *The Physics of Liquid Crystals*, Clarendon, Oxford (1974).
18. W. R. Romanko and S. H. Carr, *Macromolecules*, **21**, 2243 (1988).
19. M. Warner, *Mol. Cryst. Liq. Cryst.*, **80**, 67 (1982).
20. A. Abe and T. Yamazaki, *Macromolecules*, **22**, 2145 (1989).
21. P. J. Flory and A. Abe, *Macromolecules*, **11**(6), 1119 (1978).
22. A. Abe and P. J. Flory, *Macromolecules*, **11**(6), 1122 (1978).
23. P. J. Flory and R. S. Frost, *Macromolecules*, **11**(6), 1126 (1978).
24. R. S. Frost and P. J. Flory, *Macromolecules*, **11**(6), 1134 (1978).
25. J. Moscicki and G. Williams, *Polymer*, **23**, 558 (1982).
26. R. S. Frost, *Macromolecules*, **21**(6), 1854 (1988).
27. L. A. Chick, *Ph.D. Dissertation*, University of Washington (1990). (Available through University Microfilms, 300 North Zeeb Road, Ann Arbor, Michigan 48106.)
28. R. Alben, *Mol. Cryst. Liq. Cryst.*, **13**, 193 (1971).